

RESEARCH ARTICLE

Comparison of the miRNA expression profiles in fresh frozen and formalin-fixed paraffin-embedded tonsillar tumors

Zuzana Vojtechova^{1,2}, Jiri Zavadil³, Jan Klozar⁴, Marek Grega⁵, Ruth Tachezy^{1,2*}

1 Department of Genetics and Microbiology, Faculty of Science, Charles University, Prague, Czech Republic, **2** Department of Immunology, Institute of Hematology and Blood Transfusion, Prague, Czech Republic, **3** Molecular Mechanisms and Biomarkers Group, International Agency for Research on Cancer, Lyon, France, **4** Department of Otorhinolaryngology and Head and Neck Surgery, 1st Faculty of Medicine, Charles University, Motol University Hospital, Prague, Czech Republic, **5** Department of Pathology and Molecular Medicine, 2nd Faculty of Medicine, Charles University, Prague, Czech Republic

* ruth.tachezy@natur.cuni.cz



OPEN ACCESS

Citation: Vojtechova Z, Zavadil J, Klozar J, Grega M, Tachezy R (2017) Comparison of the miRNA expression profiles in fresh frozen and formalin-fixed paraffin-embedded tonsillar tumors. PLoS ONE 12(6): e0179645. <https://doi.org/10.1371/journal.pone.0179645>

Editor: Andre van Wijnen, University of Massachusetts Medical School, UNITED STATES

Received: December 21, 2016

Accepted: June 1, 2017

Published: June 23, 2017

Copyright: © 2017 Vojtechova et al. This is an open access article distributed under the terms of the [Creative Commons Attribution License](https://creativecommons.org/licenses/by/4.0/), which permits unrestricted use, distribution, and reproduction in any medium, provided the original author and source are credited.

Data Availability Statement: Supporting raw data were submitted to Annotare. The data are publicly available from 7/6/2017 under accession E-MTAB-5346.

Funding: The paper was supported by the Ministry of Education, Youth and Sports of CR (<http://www.msmt.cz/>) within the National Sustainability Program II (project BIOCEV-FAR) LQ1604 and by the project “BIOCEV” (CZ.1.05/1.1.00/02.0109). The funders had no role in study design, data

Abstract

MicroRNAs are considered as promising prognostic and diagnostic biomarkers of human cancer since their profiles differ between tumor types. Most of the tumor profiling studies were performed on rarely available fresh frozen (FF) samples. Alternatively, archived formalin-fixed paraffin-embedded (FFPE) tissue samples are also well applicable to larger-scale retrospective miRNA profiling studies. The aim of this study was to perform systematic comparison of the miRNA expression profiles between FF and macrodissected FFPE tonsillar tumors using the TaqMan Low Density Array system, with the data processed by different software programs and two types of normalization methods. We observed a marked correlation between the miRNA expression profiles of paired FF and FFPE samples; however, only 27–38% of the differentially deregulated miRNAs overlapped between the two source systems. The comparison of the results with regard to the distinct modes of data normalization revealed an overlap in 58–67% of differentially expressed miRNAs, with no influence of the choice of software platform. Our study highlights the fact that for an accurate comparison of the miRNA expression profiles from published studies, it is important to use the same type of clinical material and to test and select the best-performing normalization method for data analysis.

Introduction

MicroRNAs (miRNAs) are small non coding RNAs (~21 nucleotides) which play an important role in post-transcriptional regulation of gene expression. Their binding with perfect or imperfect complementarity to the 3' untranslated region of the target mRNA leads either to mRNA cleavage and degradation or to inhibition of mRNA translation [1]. Of interest, Ørom et al. also reported an association of miRNA with the 5' untranslated region which resulted in the activation of gene expression [2, 3]. MiRNAs are involved in many biological processes such as

collection and analysis, decision to publish, or preparation of the manuscript.

Competing interests: The authors have declared that no competing interests exist.

cellular development, proliferation, differentiation, survival or regulation of apoptosis. The expression of miRNAs is deregulated in human cancer. It has been reported that they can act as tumor suppressors or oncogenes based on their targets. The miRNA expression profiles are specific for malignant and non-malignant tissues, and it has been shown the miRNA profiles differ across tumor types [4]. Many studies focused on the miRNA profiling of tumor types of different origin have been published since miRNAs are considered as promising prognostic and diagnostic biomarkers of human cancer [5–7].

Most of the miRNA profiling studies of tumors were at first performed on the fresh frozen samples (FF) where the RNA is well preserved. However, this type of clinical material is rarely available. The disadvantage of formalin fixation is that it preserves the tissue by creating cross-links between all tissue and molecular components, and these modifications can cause the fragmentation of RNA [8]. However, contrary to mRNA, the stability of miRNAs is not influenced by formalin fixation, probably due to their small size and secondary structure [8–10]. Archived material, formalin-fixed paraffin-embedded tissue samples (FFPE), has proven usable for miRNA analyses and allows for retrospective large studies where the results can be correlated with clinical parameters and prognosis of patients.

Numerous studies have shown the tissue specific expression profiles as well as the differences in the abundantly expressed miRNAs in different types of tumors. However, the overlap of the lists of tumor specific miRNAs is, for most cancer types, poor. Several reasons can explain the discrepant data. One of them can be the use of different types of clinical material or of different methodological approaches.

In our previously published study [11], we found that the tumor homogeneity is important for the robustness of miRNA expression studies, especially in head and neck tumors which are very heterogeneous. Therefore, macrodissection of the FFPE samples provides benefit by increasing the homogeneity of the analyzed samples. To evaluate our previous data on FF HNC samples, we analyzed paired FF and macrodissected FFPE samples for the abundantly expressed miRNAs and the level of concordance in the profiles.

Few studies comparing miRNA expression in FF and FFPE paired samples have been published [12–14]. In the majority of microarray studies, good correlation of results was revealed (correlation coefficient up to 0.95), but the studies were either based on small groups of samples or differed in the workflow. None of these comparative studies has been conducted in head and neck tumors.

The aims of our study were to perform the miRNA expression profiling in a set of macrodissected FFPE samples, to compare the results with the miRNA profiles of paired fresh frozen tumors, and to assess differences possibly resulting from the use of different normalization methods and software for data analysis. Finally, from the analyses of FFPE samples, several differentially expressed miRNAs were selected for confirmation in a larger set of macrodissected FFPE tissues.

Materials and methods

Clinical samples

Ten cases of tonsillar tumors and five non-malignant tonsillar tissues were selected for the comparison of the miRNA expression profiles in fresh frozen and formalin-fixed paraffin embedded samples. All samples were obtained from patients treated at the Department of Otolaryngology and Head and Neck Surgery, 1st Faculty of Medicine, Charles University and Motol University Hospital in Prague. Fresh-frozen samples were already used in our recent study [11]. The signed informed consent form was obtained from all patients enrolled in this study. The study received official institutional and ethical approval from the Motol University

Hospital and Institute of Hematology and Blood Transfusion. The study set was selected based on the presence of HPV DNA and HPV E6 mRNA we defined in our previous studies [11, 15].

The sampling and tissue handling for FF samples has been described before [11, 15]. Sections of FF tumor samples were cut on a cryostat, and the number of tumor cells was determined by a pathologist. All FF samples contained more than 50% of tumor cells. FFPE samples were macrodissected as described before [11].

Processing of samples

Total RNA from all FF tissues was isolated by the miRVana kit (Life Technologies, USA) according to the manufacturer's protocol. Total RNA from FFPE samples was isolated simultaneously with DNA from four 10- μ m sections enriched for the tumor cells by macrodissection using the Ambion RecoverAll™ Total Nucleic Acid Isolation kit for FFPE according to the manufacturer's protocol (Applied Biosystems, USA). RNA concentration and quality was measured by a Nanodrop™ Spectrophotometer (Thermo Scientific, USA) and Experion chip electrophoresis (Bio-Rad, USA).

TaqMan Low Density Array (TLDA) analysis

The miRNA expression profiling was performed by the TaqMan® Array Human MicroRNA A +B Cards Set v3.0 (Life Technologies, USA) containing a total of 384 miRNA probes and controls per card. Overall, we analyzed 15 FF samples and 15 FFPE samples (five HPV-positive tumor samples, five HPV-negative tumor samples, and five non-malignant tissues of each material). For the analysis of FF samples, 1000 ng of total RNA was used for reverse transcription. In the case of FFPE samples, the input was 350 ng due to the smaller concentration of extracted RNA from FFPE samples. Total RNA of each sample was reverse transcribed using the TaqMan® MicroRNA Reverse Transcription Kit and Megaplex™ RT Primers specific for each card (both Life Technologies, USA) according to the manufacturer's protocol. The workflow without preamplification was chosen for both types of material, FF as well as FFPE samples. The TLDA cards were analyzed on the Applied Biosystems 7900HT Real-Time PCR System.

Data analysis

Each set of samples was evaluated separately, and the results were compared. For data processing and evaluation, we used the SDS 2.4 and the ExpressionSuite v1.0.1 software (Life Technologies, USA). Ct values identified by automated thresholding were exported separately for cards A and B, and the RQ (relative quantity) was calculated from the detected Ct values using the 2^{-Ct} formula. Data were further processed by the GeneSpring GX v13.1 software (Agilent), GenEx v6.1 (MultiD), and MeV v4.9 (TIGR TM4 suite) for comparison. We also applied two types of data normalization—50th percentile shift and global normalization—to perform within-sample normalization, globally across the data sets. For comparison of two groups in censored analyses, the T-test in combination with Pavlidis Template Matching (PTM) algorithm were used. In the comparison of differential abundance of miRNAs in the groups, the *P*-value ($P < 0.05$) and fold-change ($FC > 1.33$) were set. Only the miRNAs differentially expressed in at least 3/5 or 6/10 (60%) samples with measured results were considered for further analyses. The correlation was evaluated in the GraphPad InStat 3.0 tool using the Spearman nonparametric correlation.

Confirmation of microarray results

Selected miRNAs which were found to be differentially expressed by the microarrays in FFPE tonsillar tumor samples in comparison to the non-malignant tonsillar tissues were confirmed

by the individual RT qPCR using the TaqMan[®] MicroRNA Assays (Life Technologies, USA) as described recently [11]. Total RNA from five FFPE samples of non-malignant tonsils were used as a calibrator, and RNU48 served as the endogenous control. The data were analyzed in the GenEx v6.1 (MultiD) software. The $2^{-\Delta\Delta C_t}$ method was used for calculations of the fold change. The cut-off fold change was set as for the arrays to +/- 1.33 (33% fold change). T-test or Mann Whitney nonparametric test was applied depending on the data distribution. All results were statistically significant (P-value ≤ 0.05).

Results

The quality and concentration of total RNA was analyzed by a Nanodrop[™] Spectrophotometer and Experion chip electrophoresis. The RNA integrity number (RIN) was higher than seven in all FF samples. As documented in Fig 1, total RNA isolated from FFPE samples showed characteristic profiles for degraded RNA fragments (RIN in the range 1.9–2.6), but fragments with a length of around 200 bp were present allowing for a miRNA expression analyses.

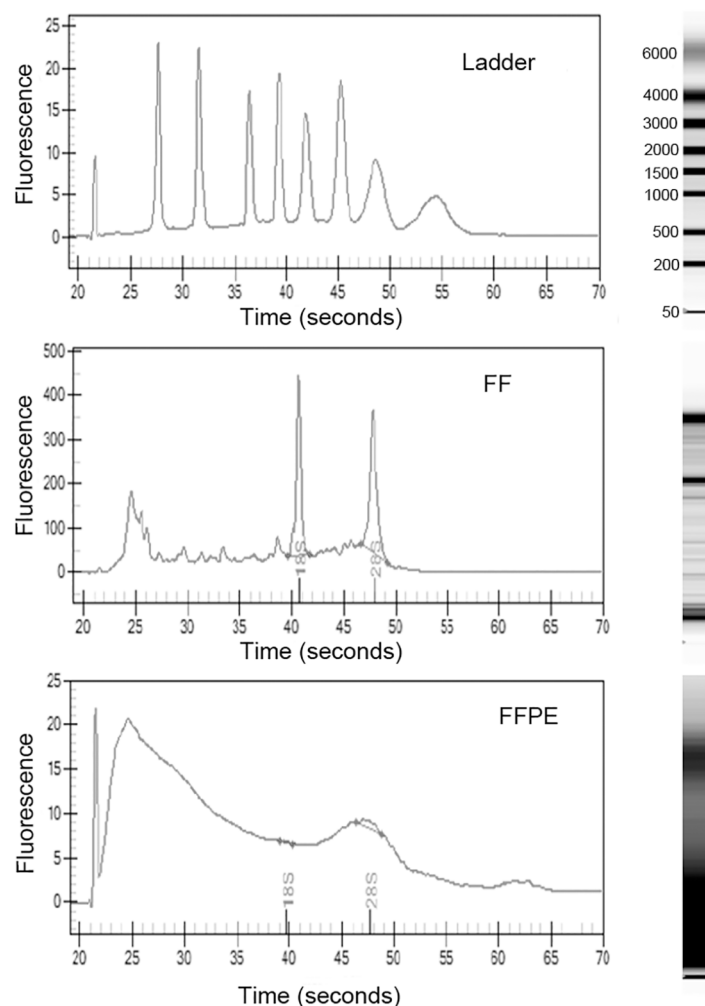


Fig 1. Comparison of electropherogram outputs. At the top—ladder, in the middle—fresh frozen sample, at the bottom—formalin-fixed paraffin-embedded sample. Right—lines from virtual gel.

<https://doi.org/10.1371/journal.pone.0179645.g001>

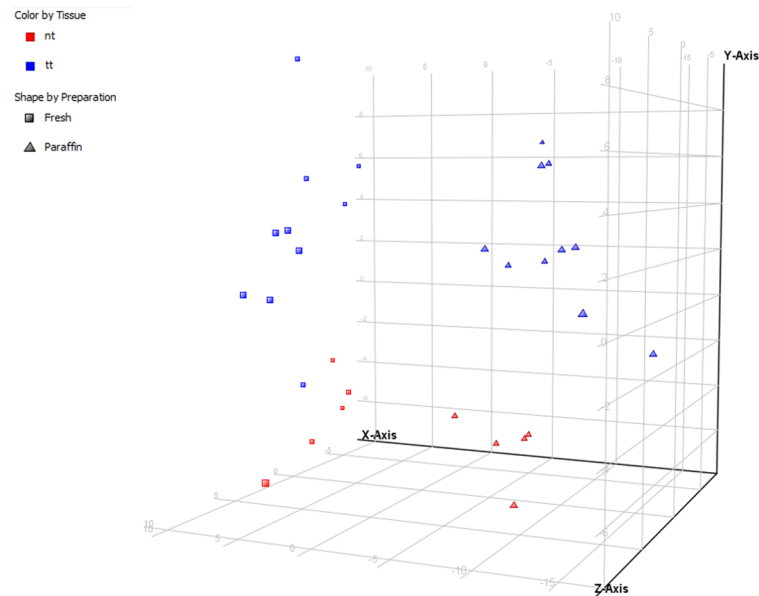


Fig 2. Principal component analysis plot. Visualization of the miRNA expression in fresh frozen (squares) and formalin-fixed paraffin-embedded (triangles) samples, as well as miRNA expression separation of tumor (blue) and non-malignant samples (red).

<https://doi.org/10.1371/journal.pone.0179645.g002>

As illustrated by the principal component analysis (PCA) (Fig 2), the miRNA expression profiles of all samples differ depending on the analyzed type of material (FF vs FFPE) and characteristics of the tissue, tumor vs normal tissue (TT vs NT). The correlation between the miRNA expression profiles of paired FF and FFPE samples was evaluated using the Spearman correlation test. The correlation of the expression level for the well characterized miRNAs located on card A was better (correlation coefficient ≥ 0.65 in 7/10 samples ($p < 0.0001$)) in comparison to all analyzed miRNAs (miRNAs on cards A and B). The exact Spearman correlation values of each comparison and the confidence intervals are summarized in Table 1. The correlation of paired samples is also visualized in scatter plots (Fig 3). Our assumption that FF samples with higher percentage of tumor cells would be more likely to give better correlation of the expression miRNA profiles with FFPE macrodissected samples was not proven. The correlation coefficient of the miRNA expression profiles of FF and FFPE samples was not influenced by the number of tumor cells in the particular FF sample (Table 1).

Differentially expressed miRNAs were identified by the P -value ($P < 0.05$) and fold-change > 1.33 with the 50th percentile shift normalization method using the GeneSpring software. In our study, macrodissected FFPE samples revealed less differentially expressed miRNAs ($N = 58$) than paired fresh frozen tumors ($N = 83$ miRNAs). When comparing the lists of deregulated miRNAs between FF and FFPE samples, we detected overlaps in 27–38% (Table 2, on the left).

To establish how the method used for normalization influences the final results, we applied, besides the 50th percentile shift normalization, also global normalization for each group of the analyzed samples. As illustrated in Fig 4 and Table 3, the differentially expressed miRNAs based on each normalization method overlap in 58–67% for FF and/or FFPE samples. Using different software and the identical normalization method, almost 90% of the deregulated miRNAs were concordant between FF and FFPE samples (data not shown).

Table 1. Spearman correlation values between miRNA expression profiles of FF and FFPE paired samples.

Sample		R	CI	tumor cells in FF (%)
FF 102 vs FFPE 58	card A	0,6982	0,6199 to 0,7628	> 50%
	card A+B	0,5848	0,5088 to 0,6517	
FF 116 vs FFPE 1	card A	0,5194	0,4064 to 0,6167	> 70%
	card A+B	0,4642	0,3698 to 0,5491	
FF 148 vs FFPE 60	card A	0,7406	0,6757 to 0,7941	> 70%
	card A+B	0,6749	0,6150 to 0,7271	
FF 161 vs FFPE 13	card A	0,8302	0,7829 to 0,8680	> 60%
	card A+B	0,7174	0,6632 to 0,7641	
FF 174 vs FFPE 49	card A	0,6378	0,5500 to 0,7117	> 50%
	card A+B	0,5748	0,4999 to 0,6412	
FF 183 vs FFPE 62	card A	0,6905	0,6098 to 0,7570	70%
	card A+B	0,6373	0,5664 to 0,6989	
FF 187 vs FFPE 30	card A	0,5879	0,4883 to 0,6724	> 70%
	card A+B	0,5152	0,4289 to 0,5922	
FF 191 vs FFPE 63	card A	0,7332	0,6648 to 0,7894	> 80%
	card A+B	0,6593	0,5959 to 0,7145	
FF 137 vs FFPE 6	card A	0,7914	0,7363 to 0,8360	90%
	card A+B	0,7361	0,6828 to 0,7816	
FF 224 vs FFPE 22	card A	0,7371	0,6697 to 0,7925	80%
	card A+B	0,7124	0,6571 to 0,7601	

<https://doi.org/10.1371/journal.pone.0179645.t001>

We performed additional analysis and identified 16 miRNAs commonly detected in both type of material and using both type of normalization (Table 4). These miRNAs were screened in database miRSearch V3.0 (Exiqon). Most of them have experimentally proved target genes participating in signaling pathways and cellular processes including not only tumor development. Noteworthy, target genes are transcription factors E2F, MAP kinases, members of RAS protein family, tumor suppressor PTEN, transforming growth factors TGFs, tumor suppressor TP53, proteins participating in cell cycle (cyclins, cyclin-dependent kinases) or regulating cell death.

Finally, from the deregulated miRNAs in FFPE samples, we have selected 11 tumor-specific miRNAs, also with regard to viral or non-viral etiology of the tumor. The expression of these miRNAs was evaluated in a larger set of 64 macrodissected tumor samples by individual Taq-Man assays (Fig 5). MiR-106b# and miR-9 were selected as specific for HPV-positive tonsillar tumors, miR-16, miR-34a, miR-193b, miR-31, miR-221, and miR-21 as specific for HPV-negative tumors, and miR-155, miR-126, and miR-205 as specific for tonsillar tumors of any etiology. The differential expression of six miRNAs (miR-106b#, miR-9, miR-16, miR-34a, miR-155, and miR-126) ($P < 0.05$; $FC > 1.33$) was confirmed in a larger set of 64 tumor samples, the fold change of miR-193b was equal to 1.23, but the trend of expression was also maintained. The trend of expression of four miRNAs (miR-31, miR-221, miR-21, and miR-205) analyzed in the large set of samples was opposite to that derived from the results revealed by arrays.

Discussion

The archives of formalin-fixed paraffin-embedded material in pathology laboratories offer the possibility to analyze the samples retrospectively and provide the option for clinical cancer research to extend the studies, and, moreover, to correlate the results with clinical data

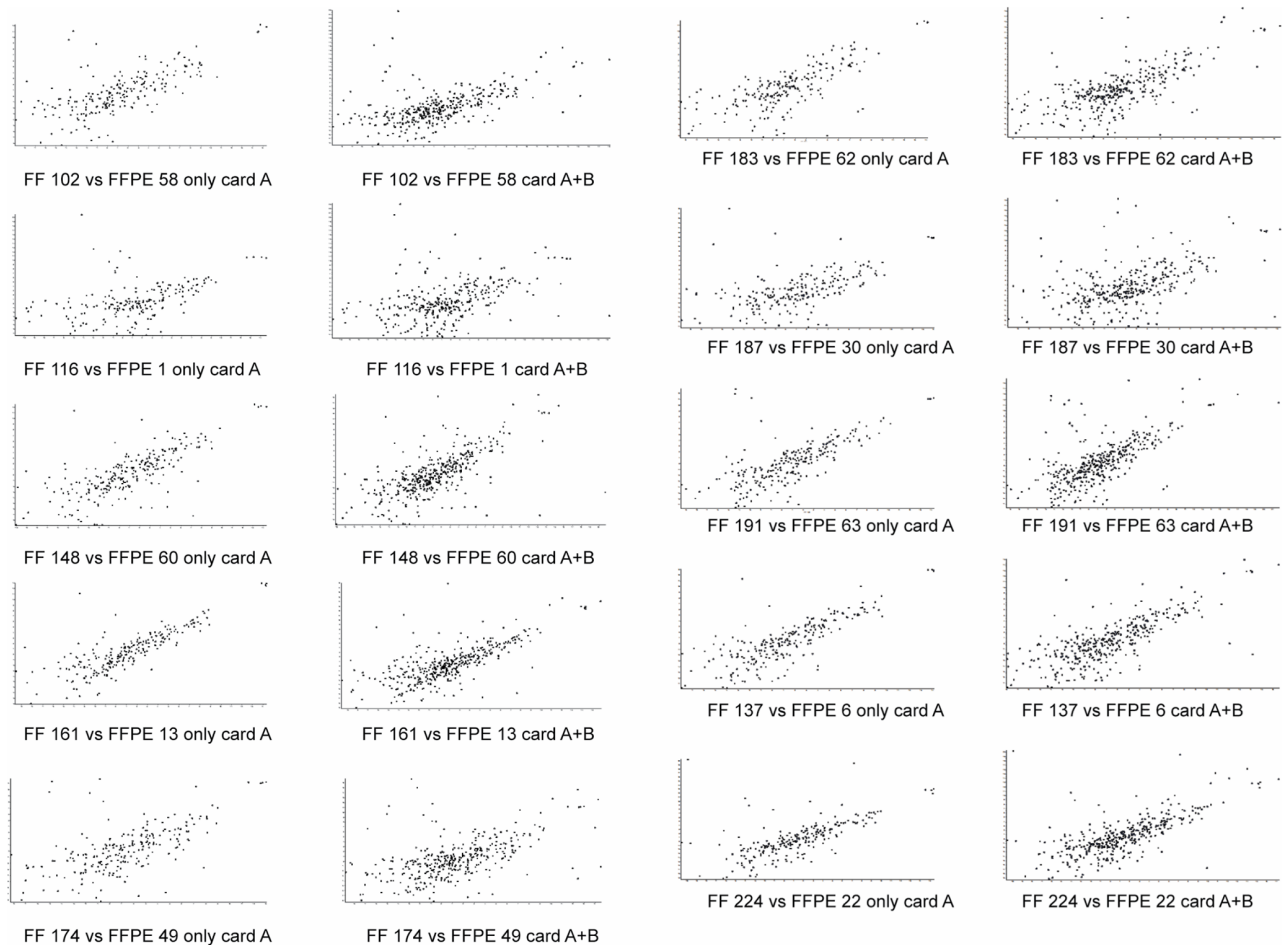


Fig 3. Correlation of paired samples visualized on scatterplots. Scatter plots of the normalized RQ values in pair-wise comparison from fresh-frozen (FF) and formalin-fixed paraffin embedded (FFPE) samples.

<https://doi.org/10.1371/journal.pone.0179645.g003>

obtained during long-term follow-up of patients. The utilization of FFPE material for RNA based studies is still challenging, especially due to RNA fragmentation. However, the small size of miRNAs contributes to their stability during the processing of FFPE samples [9] so that FFPE tissues are applicable for miRNA expression analysis studies as previously shown [16–19]. Chatterjee et al. have presented a cross comparison of miRNA detection technologies in FFPE samples and revealed that it is possible to obtain high quality sequence reads for miRNA profiling in FFPE samples with an RNA integrity number around 2 [20].

In our study, we performed the miRNA expression profiling by TLDA analysis in a set of macrodissected FFPE samples and compared the results with the miRNA expression profiles of paired fresh frozen samples. Most studies comparing the miRNA expression between FF and FFPE samples were performed using only several selected miRNAs [21–25].

A comparison of the miRNA expression profiles in FF and FFPE samples obtained by the microarray analysis has also been published. Romero-Cordoba et al. have performed a comparative analysis of paired samples of breast cancer using the TaqMan Low Density Array platform, similarly to Hui et al. [12, 14]. They revealed a high correlation; however, both studies analyzed small groups of paired samples and did not use dissected samples. Goswami et al. have also observed a high correlation between the samples; however, their workflow differed

Table 2. Differentially expressed miRNAs detected in tonsillar tumors versus non-malignant tonsillar tissue. The overlap between FF vs FFPE material is highlighted in green. On the left—results using 50th percentile shift normalization for data analysis. On the right—results using global normalization for data analysis. FC—fold change.

50th percentile shift normalization				global normalization			
FF		FFPE		FF		FFPE	
TTall vs NT				TTall vs NT			
miRNA	FC	miRNA	FC	miRNA	FC	miRNA	FC
hsa-miR-101-002253	-2.87	hsa-miR-101-002253	-8.70	hsa-let-7g-002282	-1.85	hsa-let-7g-002282	-2.57
hsa-miR-126#-000451	-2.29	hsa-miR-126#-000451	-8.27	hsa-miR-126#-000451	-1.85	hsa-miR-126#-000451	-4.28
hsa-miR-130b-000456	1.86	hsa-miR-130b-000456	3.42	hsa-miR-140-3p-002234	-2.10	hsa-miR-140-3p-002234	-4.50
hsa-miR-140-3p-002234	-2.42	hsa-miR-140-3p-002234	-4.15	hsa-miR-141-000463	4.71	hsa-miR-141-000463	3.85
hsa-miR-141-000463	4.04	hsa-miR-141-000463	2.67	hsa-miR-143-002249	-2.14	hsa-miR-143-002249	-1.68
hsa-miR-142-3p-000464	-3.85	hsa-miR-142-3p-000464	-8.79	hsa-miR-144#-002148	-4.52	hsa-miR-144#-002148	-2.95
hsa-miR-143-002249	-2.02	hsa-miR-143-002249	-2.89	hsa-miR-184-000485	-6.15	hsa-miR-184-000485	-5.46
hsa-miR-195-000494	-1.92	hsa-miR-195-000494	-2.89	hsa-miR-196b-002215	7.00	hsa-miR-196b-002215	2.88
hsa-miR-196b-002215	8.26	hsa-miR-196b-002215	4.42	hsa-miR-200a-000502	3.52	hsa-miR-200a-000502	3.32
hsa-miR-200b-002251	3.86	hsa-miR-200b-002251	2.60	hsa-miR-200b-002251	3.04	hsa-miR-200b-002251	2.89
hsa-miR-200c-002300	3.45	hsa-miR-200c-002300	3.00	hsa-miR-200c-002300	2.83	hsa-miR-200c-002300	3.33
hsa-miR-205-000509	4.22	hsa-miR-205-000509	5.12	hsa-miR-205-000509	4.58	hsa-miR-205-000509	6.71
hsa-miR-21#-002438	2.99	hsa-miR-21#-002438	2.53	hsa-miR-210-000512	3.74	hsa-miR-210-000512	3.26
hsa-miR-210-000512	4.10	hsa-miR-210-000512	2.70	hsa-miR-224-002099	5.62	hsa-miR-224-002099	5.78
hsa-miR-221-000524	2.69	hsa-miR-221-000524	2.70	hsa-miR-27a#-002445	4.10	hsa-miR-27a#-002445	2.79
hsa-miR-224-002099	6.01	hsa-miR-224-002099	6.03	hsa-miR-27a-000408	2.19	hsa-miR-27a-000408	1.80
hsa-miR-27a#-002445	3.12	hsa-miR-27a#-002445	4.47	hsa-miR-29a-002112	-1.61	hsa-miR-29a-002112	-2.57
hsa-miR-27a-000408	1.81	hsa-miR-27a-000408	1.92	hsa-miR-429-001024	3.25	hsa-miR-429-001024	2.37
hsa-miR-29a-002112	-1.83	hsa-miR-29a-002112	-3.26	hsa-miR-452-002329	2.79	hsa-miR-452-002329	1.89
hsa-miR-452-002329	3.00	hsa-miR-452-002329	3.84	hsa-miR-484-001821	2.02	hsa-miR-484-001821	2.40
hsa-miR-486-3p-002093	-3.79	hsa-miR-486-3p-002093	-4.97	hsa-miR-886-3p-002194	3.04	hsa-miR-886-3p-002194	2.94
hsa-miR-886-3p-002194	3.00	hsa-miR-886-3p-002194	2.59	hsa-let-7i#-002172	-2.59	hsa-miR-106b-000442	1.94
hsa-miR-100-000437	-1.62	hsa-let-7b#-002404	-6.10	hsa-miR-100-000437	-1.88	hsa-miR-1253-002894	11.36
hsa-miR-1180-002847	3.95	hsa-let-7g-002282	-3.04	hsa-miR-101-002253	-2.43	hsa-miR-1260-002896	1.58
hsa-miR-1227-002769	4.37	hsa-miR-126-002228	-3.28	hsa-miR-1244-002791	2.49	hsa-miR-126-002228	-2.95
hsa-miR-125b-000449	-1.93	hsa-miR-1262-002852	-10500.89	hsa-miR-125b-000449	-2.44	hsa-miR-127-000452	3.13
hsa-miR-132-000457	1.66	hsa-miR-127-000452	2.01	hsa-miR-132-000457	1.75	hsa-miR-1282-002803	1.35
hsa-miR-135b#-002159	5.18	hsa-miR-138-002284	-3.48	hsa-miR-135b-002261	4.30	hsa-miR-130b-000456	3.51
hsa-miR-135b-002261	4.25	hsa-miR-146a-000468	-3.45	hsa-miR-138-002284	-3.48	hsa-miR-142-3p-000464	-5.87
hsa-miR-136#-002100	-3.36	hsa-miR-146b-001097	-2.48	hsa-miR-139-5p-002289	-3.48	hsa-miR-142-5p-002248	-2.40
hsa-miR-139-3p-002313	-2.80	hsa-miR-150-000473	-10.82	hsa-miR-141#-002145	2.64	hsa-miR-146a-000468	-2.75
hsa-miR-139-5p-002289	-2.97	hsa-miR-155-002623	-3.39	hsa-miR-145#-002149	-2.09	hsa-miR-146b-001097	-2.25
hsa-miR-144#-002148	-5.50	hsa-miR-15a-000389	-2.18	hsa-miR-145-002278	-2.28	hsa-miR-150-000473	-8.31
hsa-miR-145#-002149	-2.55	hsa-miR-16-000391	-2.58	hsa-miR-146b-3p-002361	1.29	hsa-miR-152-000475	2.37
hsa-miR-145-002278	-2.60	hsa-miR-188-3p-002106	-15.67	hsa-miR-151-3p-002254	1.69	hsa-miR-155-002623	-3.37
hsa-miR-181a-000480	-1.50	hsa-miR-19a-000395	-2.14	hsa-miR-151-5P-002642	-1.96	hsa-miR-16-000391	-2.23
hsa-miR-182-002334	3.36	hsa-miR-19b-000396	-2.64	hsa-miR-15b#-002173	4.90	hsa-miR-183#-002270	1.77
hsa-miR-1825-002907	8.50	hsa-miR-20a#-002437	-4.90	hsa-miR-15b-000390	1.89	hsa-miR-18a#-002423	1.84
hsa-miR-183-002269	2.77	hsa-miR-21-000397	1.49	hsa-miR-181a-000480	-1.64	hsa-miR-19b-000396	-2.58
hsa-miR-184-000485	-22.46	hsa-miR-213-000516	-4.21	hsa-miR-183-002269	2.49	hsa-miR-20a#-002437	-2.15
hsa-miR-191#-002678	4.11	hsa-miR-219-2-3p-002390	26.64	hsa-miR-195-000494	-2.33	hsa-miR-21#-002438	2.58
hsa-miR-197-000497	1.72	hsa-miR-323-3p-002227	5.88	hsa-miR-199a-3p-002304	-1.59	hsa-miR-213-000516	-3.40
hsa-miR-200a#-001011	3.42	hsa-miR-342-3p-002260	-3.35	hsa-miR-200a#-001011	4.35	hsa-miR-221-000524	2.86

(Continued)

Table 2. (Continued)

50th percentile shift normalization				global normalization			
FF		FFPE		FF		FFPE	
TTall vs NT				TTall vs NT			
miRNA	FC	miRNA	FC	miRNA	FC	miRNA	FC
hsa-miR-200a-000502	3.64	hsa-miR-342-5p-002147	-3.96	hsa-miR-21#-002438	3.76	hsa-miR-223#-002098	-2.63
hsa-miR-204-000508	-5.28	hsa-miR-362-001273	2.43	hsa-miR-21-000397	2.68	hsa-miR-299-5p-000600	4.75
hsa-miR-211-000514	34.58	hsa-miR-374-000563	-2.24	hsa-miR-214#-002293	-1.74	hsa-miR-320-002277	1.92
hsa-miR-222#-002097	2.09	hsa-miR-423-5p-002340	-5.05	hsa-miR-222#-002097	2.38	hsa-miR-323-3p-002227	4.17
hsa-miR-24-000402	1.59	hsa-miR-455-3p-002244	7.08	hsa-miR-222-002276	2.04	hsa-miR-342-3p-002260	-3.14
hsa-miR-26a-000405	-2.12	hsa-miR-485-3p-001277	3.99	hsa-miR-24-000402	1.73	hsa-miR-362-001273	2.07
hsa-miR-26b#-002444	-5.11	hsa-miR-490-001037	3.37	hsa-miR-26a-000405	-1.84	hsa-miR-455-3p-002244	8.08
hsa-miR-26b-000407	-2.22	hsa-miR-516-3p-001149	-12.45	hsa-miR-26b#-002444	-3.16	hsa-miR-485-3p-001277	2.33
hsa-miR-27b#-002174	1.88	hsa-miR-566-001533	-4.10	hsa-miR-26b-000407	-2.85	hsa-miR-532-001518	-2.24
hsa-miR-29a#-002447	-2.62	hsa-miR-583-001623	12.93	hsa-miR-29a#-002447	-1.98	hsa-miR-550-002410	-2.05
hsa-miR-29b-000413	-2.17	hsa-miR-590-5p-001984	-6.36	hsa-miR-29b-000413	-2.45	hsa-miR-590-5p-001984	-2.27
hsa-miR-29c-000587	-2.39	hsa-miR-640-001584	-4.53	hsa-miR-29c-000587	-2.64	hsa-miR-629-001562	-2.19
hsa-miR-302a-000529	222.12	hsa-miR-660-001515	-1.96	hsa-miR-302c-000533	18.15	hsa-miR-663B-002857	1.78
hsa-miR-30a-3p-000416	-3.27	hsa-miR-663B-002857	2.55	hsa-miR-30b-000602	-1.76	hsa-miR-888-002212	-551.31
hsa-miR-30a-5p-000417	-1.93	hsa-miR-942-002187	-3.76	hsa-miR-30d-000420	-1.95		
hsa-miR-30d-000420	-1.94			hsa-miR-31-002279	6.09		
hsa-miR-30e-3p-000422	-2.39			hsa-miR-32-002109	-2.47		
hsa-miR-31-002279	5.72			hsa-miR-335#-002185	2.58		
hsa-miR-335#-002185	2.04			hsa-miR-342-5p-002147	-7.89		
hsa-miR-335-000546	2.33			hsa-miR-34b-002102	2.35		
hsa-miR-34a#-002316	1.91			hsa-miR-505#-002087	-1.68		
hsa-miR-378-000567	-1.87			hsa-miR-511-001111	2.16		
hsa-miR-429-001024	3.66			hsa-miR-520g-001121	3.52		
hsa-miR-431-001979	16.66			hsa-miR-577-002675	-3.38		
hsa-miR-484-001821	2.01			hsa-miR-596-001550	-2.00		
hsa-miR-486-001278	-3.26			hsa-miR-649-001602	3.05		
hsa-miR-497-001043	-4.12			hsa-miR-708-002341	2.14		
hsa-miR-505#-002087	-2.84			hsa-miR-944-002189	5.27		
hsa-miR-511-001111	3.25			hsa-miR-9-000583	7.17		
hsa-miR-517a-002402	3.23						
hsa-miR-517c-001153	3.66						
hsa-miR-523-002386	10.93						
hsa-miR-576-3p-002351	8.52						
hsa-miR-627-001560	29.22						
hsa-miR-643-001594	2.71						
hsa-miR-658-001513	2.12						
hsa-miR-659-001514	6.10						
hsa-miR-708-002341	2.26						
hsa-miR-944-002189	6.72						
hsa-miR-99b#-002196	-4.26						
22/83 (27%)		22/58 (38%)		21/72 (29%)		21/57 (37%)	

<https://doi.org/10.1371/journal.pone.0179645.t002>

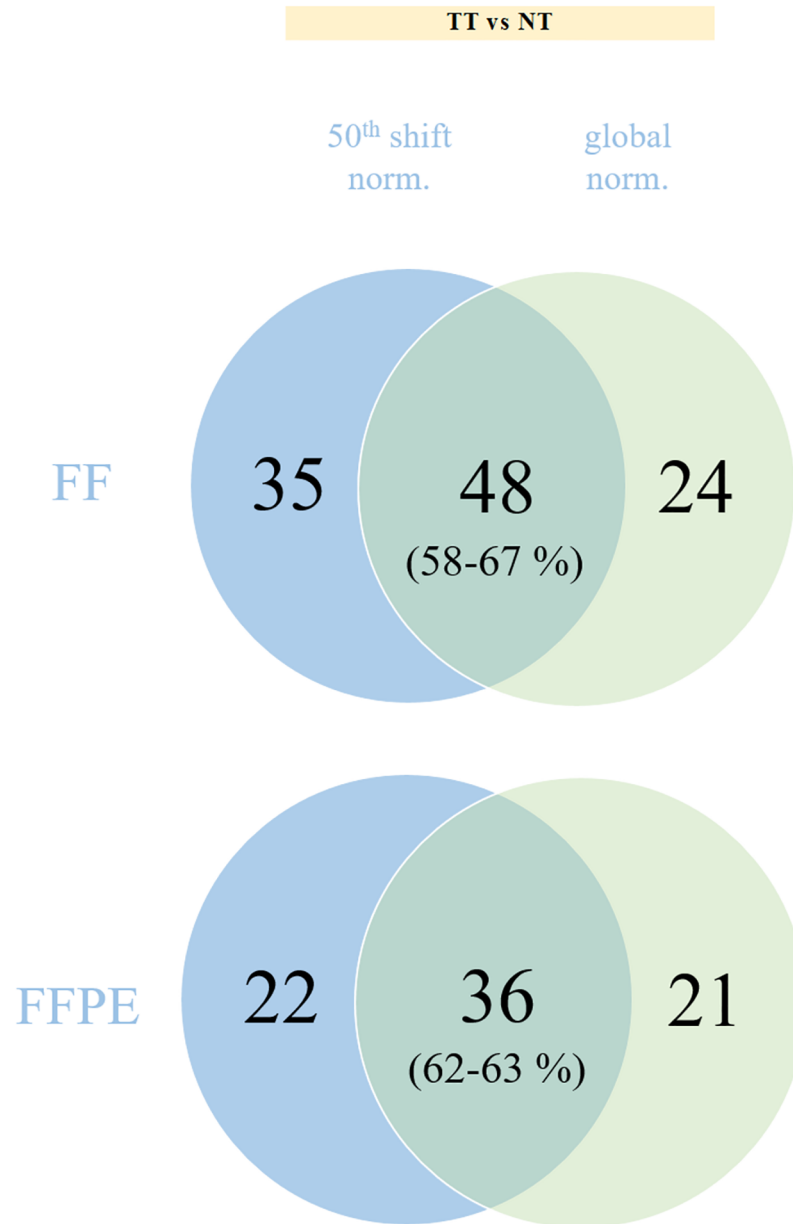


Fig 4. Comparison of differentially expressed miRNAs. Comparison of differentially expressed miRNAs identified using 50th percentile shift normalization and global normalization for each clinical material.

<https://doi.org/10.1371/journal.pone.0179645.g004>

in several aspects (assessment of extraction method, platform optimization, etc.) [13]. Additional studies were performed using other microarray platforms [9, 26, 27] or next generation sequencing platforms [28]. None of this comparative studies has been performed in head and neck tumors.

Since our recent study has shown that the tumor tissue homogeneity is important for the robustness of the miRNA profiling studies, we performed macrodissection of FFPE samples to enrich them for tumor cells. To our knowledge, only one study dealt with the issue of FFPE dissection. It tested the possibility of a non-satisfactory correlation of the expression of several miRNAs between FF and dissected FFPE samples due to the enrichment of the tumor cells.

Table 3. Differentially expressed miRNAs detected tonsillar tumors versus non-malignant tonsillar tissue. Overlap between results using 50th percentile shift normalization and global normalization is highlighted in green. On the left—results from FF samples, on the right—results from FFPE samples. FC—fold change.

FF				FFPE			
TTall vs NT				TTall vs NT			
50th percentile shift normalization		global normalization		50th percentile shift normalization		global normalization	
miRNA	FC	miRNA	FC	miRNA	FC	miRNA	FC
hsa-miR-100-000437	-1.62	hsa-miR-100-000437	-1.88	hsa-let-7g-002282	-3.04	hsa-let-7g-002282	-2.57
hsa-miR-101-002253	-2.87	hsa-miR-101-002253	-2.43	hsa-miR-126#-000451	-8.27	hsa-miR-126#-000451	-4.28
hsa-miR-125b-000449	-1.93	hsa-miR-125b-000449	-2.44	hsa-miR-126-002228	-3.28	hsa-miR-126-002228	-2.95
hsa-miR-126#-000451	-2.29	hsa-miR-126#-000451	-1.85	hsa-miR-127-000452	2.01	hsa-miR-127-000452	3.13
hsa-miR-132-000457	1.66	hsa-miR-132-000457	1.75	hsa-miR-130b-000456	3.42	hsa-miR-130b-000456	3.51
hsa-miR-135b-002261	4.25	hsa-miR-135b-002261	4.30	hsa-miR-140-3p-002234	-4.15	hsa-miR-140-3p-002234	-4.50
hsa-miR-139-5p-002289	-2.97	hsa-miR-139-5p-002289	-3.48	hsa-miR-141-000463	2.67	hsa-miR-141-000463	3.85
hsa-miR-140-3p-002234	-2.42	hsa-miR-140-3p-002234	-2.10	hsa-miR-142-3p-000464	-8.79	hsa-miR-142-3p-000464	-5.87
hsa-miR-141-000463	4.04	hsa-miR-141-000463	4.71	hsa-miR-143-002249	-2.89	hsa-miR-143-002249	-1.68
hsa-miR-143-002249	-2.02	hsa-miR-143-002249	-2.14	hsa-miR-146a-000468	-3.45	hsa-miR-146a-000468	-2.75
hsa-miR-144#-002148	-5.50	hsa-miR-144#-002148	-4.52	hsa-miR-146b-001097	-2.48	hsa-miR-146b-001097	-2.25
hsa-miR-145#-002149	-2.55	hsa-miR-145#-002149	-2.09	hsa-miR-150-000473	-10.82	hsa-miR-150-000473	-8.31
hsa-miR-145-002278	-2.60	hsa-miR-145-002278	-2.28	hsa-miR-155-002623	-3.39	hsa-miR-155-002623	-3.37
hsa-miR-181a-000480	-1.50	hsa-miR-181a-000480	-1.64	hsa-miR-16-000391	-2.58	hsa-miR-16-000391	-2.23
hsa-miR-183-002269	2.77	hsa-miR-183-002269	2.49	hsa-miR-196b-002215	4.42	hsa-miR-196b-002215	2.88
hsa-miR-184-000485	-22.46	hsa-miR-184-000485	-6.15	hsa-miR-19b-000396	-2.64	hsa-miR-19b-000396	-2.58
hsa-miR-195-000494	-1.92	hsa-miR-195-000494	-2.33	hsa-miR-200b-002251	2.60	hsa-miR-200b-002251	2.89
hsa-miR-196b-002215	8.26	hsa-miR-196b-002215	7.00	hsa-miR-200c-002300	3.00	hsa-miR-200c-002300	3.33
hsa-miR-200a#-001011	3.42	hsa-miR-200a#-001011	4.35	hsa-miR-205-000509	5.12	hsa-miR-205-000509	6.71
hsa-miR-200a-000502	3.64	hsa-miR-200a-000502	3.52	hsa-miR-20a#-002437	-4.90	hsa-miR-20a#-002437	-2.15
hsa-miR-200b-002251	3.86	hsa-miR-200b-002251	3.04	hsa-miR-21#-002438	2.53	hsa-miR-21#-002438	2.58
hsa-miR-200c-002300	3.45	hsa-miR-200c-002300	2.83	hsa-miR-210-000512	2.70	hsa-miR-210-000512	3.26
hsa-miR-205-000509	4.22	hsa-miR-205-000509	4.58	hsa-miR-213-000516	-4.21	hsa-miR-213-000516	-3.40
hsa-miR-21#-002438	2.99	hsa-miR-21#-002438	3.76	hsa-miR-221-000524	2.90	hsa-miR-221-000524	2.86
hsa-miR-210-000512	4.10	hsa-miR-210-000512	3.74	hsa-miR-224-002099	6.03	hsa-miR-224-002099	5.78
hsa-miR-222#-002097	2.09	hsa-miR-222#-002097	2.38	hsa-miR-27a#-002445	4.47	hsa-miR-27a#-002445	2.79
hsa-miR-224-002099	6.01	hsa-miR-224-002099	5.62	hsa-miR-27a-000408	1.92	hsa-miR-27a-000408	1.80
hsa-miR-24-000402	1.59	hsa-miR-24-000402	1.73	hsa-miR-29a-002112	-3.26	hsa-miR-29a-002112	-2.57
hsa-miR-26a-000405	-2.12	hsa-miR-26a-000405	-1.84	hsa-miR-323-3p-002227	5.88	hsa-miR-323-3p-002227	4.17
hsa-miR-26b#-002444	-5.11	hsa-miR-26b#-002444	-3.16	hsa-miR-342-3p-002260	-3.35	hsa-miR-342-3p-002260	-3.14
hsa-miR-26b-000407	-2.22	hsa-miR-26b-000407	-2.85	hsa-miR-362-001273	2.43	hsa-miR-362-001273	2.07
hsa-miR-27a#-002445	3.12	hsa-miR-27a#-002445	4.10	hsa-miR-452-002329	3.84	hsa-miR-452-002329	1.90
hsa-miR-27a-000408	1.81	hsa-miR-27a-000408	2.19	hsa-miR-455-3p-002244	7.08	hsa-miR-455-3p-002244	8.08
hsa-miR-29a#-002447	-2.62	hsa-miR-29a#-002447	-1.98	hsa-miR-485-3p-001277	3.99	hsa-miR-485-3p-001277	2.33
hsa-miR-29a-002112	-1.83	hsa-miR-29a-002112	-1.61	hsa-miR-590-5p-001984	-6.36	hsa-miR-590-5p-001984	-2.27
hsa-miR-29b-000413	-2.17	hsa-miR-29b-000413	-2.45	hsa-miR-886-3p-002194	2.59	hsa-miR-886-3p-002194	2.94
hsa-miR-29c-000587	-2.39	hsa-miR-29c-000587	-2.64	hsa-let-7b#-002404	-6.10	hsa-miR-106b-000442	1.94
hsa-miR-30d-000420	-1.94	hsa-miR-30d-000420	-1.95	hsa-miR-101-002253	-8.70	hsa-miR-1253-002894	11.36
hsa-miR-31-002279	5.72	hsa-miR-31-002279	6.09	hsa-miR-1262-002852	-10500.89	hsa-miR-1260-002896	1.58
hsa-miR-335#-002185	2.04	hsa-miR-335#-002185	2.58	hsa-miR-138-002284	-3.48	hsa-miR-1282-002803	1.35
hsa-miR-429-001024	3.66	hsa-miR-429-001024	3.25	hsa-miR-15a-000389	-2.18	hsa-miR-142-5p-002248	-2.40
hsa-miR-452-002329	3.00	hsa-miR-452-002329	2.79	hsa-miR-188-3p-002106	-15.67	hsa-miR-144#-002148	-2.95

(Continued)

Table 3. (Continued)

FF				FFPE			
TTall vs NT				TTall vs NT			
50th percentile shift normalization		global normalization		50th percentile shift normalization		global normalization	
miRNA	FC	miRNA	FC	miRNA	FC	miRNA	FC
hsa-miR-484-001821	2.01	hsa-miR-484-001821	2.02	hsa-miR-195-000494	-2.89	hsa-miR-152-000475	2.3
hsa-miR-505#-002087	-2.84	hsa-miR-505#-002087	-1.68	hsa-miR-19a-000395	-2.14	hsa-miR-183#-002270	1.77
hsa-miR-511-001111	3.25	hsa-miR-511-001111	2.16	hsa-miR-21-000397	1.49	hsa-miR-184-000485	-5.46
hsa-miR-708-002341	2.26	hsa-miR-708-002341	2.14	hsa-miR-219-2-3p-002390	26.64	hsa-miR-18a#-002423	1.84
hsa-miR-886-3p-002194	3.00	hsa-miR-886-3p-002194	3.04	hsa-miR-342-5p-002147	-3.96	hsa-miR-200a-000502	3.32
hsa-miR-944-002189	6.72	hsa-miR-944-002189	7.17	hsa-miR-374-000563	-2.24	hsa-miR-223#-002098	-2.63
hsa-miR-1180-002847	3.95	hsa-let-7g-002282	-1.85	hsa-miR-423-5p-002340	-5.05	hsa-miR-299-5p-000600	4.75
hsa-miR-1227-002769	4.37	hsa-let-7i#-002172	-2.59	hsa-miR-486-3p-002093	-4.97	hsa-miR-320-002277	1.92
hsa-miR-130b-000456	1.86	hsa-miR-1244-002791	2.49	hsa-miR-490-001037	3.37	hsa-miR-429-001024	2.37
hsa-miR-135b#-002159	5.18	hsa-miR-138-002284	-3.48	hsa-miR-516-3p-001149	-12.45	hsa-miR-484-001821	2.40
hsa-miR-136#-002100	-3.36	hsa-miR-141#-002145	2.64	hsa-miR-566-001533	-4.10	hsa-miR-532-001518	-2.24
hsa-miR-139-3p-002313	-2.80	hsa-miR-146b-3p-002361	1.29	hsa-miR-583-001623	12.93	hsa-miR-550-002410	-2.05
hsa-miR-142-3p-000464	-3.85	hsa-miR-151-3p-002254	1.69	hsa-miR-640-001584	-4.53	hsa-miR-629-001562	-2.19
hsa-miR-182-002334	3.36	hsa-miR-151-5P-002642	-1.96	hsa-miR-660-001515	-1.96	hsa-miR-663B-002857	1.78
hsa-miR-1825-002907	8.50	hsa-miR-15b#-002173	4.90	hsa-miR-663B-002857	2.55	hsa-miR-888-002212	-551.31
hsa-miR-191#-002678	4.11	hsa-miR-15b-000390	1.89	hsa-miR-942-002187	-3.76		
hsa-miR-197-000497	1.72	hsa-miR-199a-3p-002304	-1.59				
hsa-miR-204-000508	-5.28	hsa-miR-21-000397	2.68				
hsa-miR-211-000514	34.58	hsa-miR-214#-002293	-1.74				
hsa-miR-221-000524	2.69	hsa-miR-222-002276	2.04				
hsa-miR-27b#-002174	1.88	hsa-miR-302c-000533	18.15				
hsa-miR-302a-000529	222.12	hsa-miR-30b-000602	-1.76				
hsa-miR-30a-3p-000416	-3.27	hsa-miR-32-002109	-2.47				
hsa-miR-30a-5p-000417	-1.93	hsa-miR-342-5p-002147	-7.89				
hsa-miR-30e-3p-000422	-2.39	hsa-miR-34b-002102	2.35				
hsa-miR-335-000546	2.33	hsa-miR-520g-001121	3.52				
hsa-miR-34a#-002316	1.91	hsa-miR-577-002675	-3.38				
hsa-miR-378-000567	-1.87	hsa-miR-596-001550	-2.00				
hsa-miR-431-001979	16.66	hsa-miR-649-001602	3.05				
hsa-miR-486-001278	-3.26	hsa-miR-9-000583	5.27				
hsa-miR-486-3p-002093	-3.79						
hsa-miR-497-001043	-4.12						
hsa-miR-517a-002402	3.23						
hsa-miR-517c-001153	3.66						
hsa-miR-523-002386	10.93						
hsa-miR-576-3p-002351	8.52						
hsa-miR-627-001560	29.22						
hsa-miR-643-001594	2.71						
hsa-miR-658-001513	2.12						
hsa-miR-659-001514	6.10						
hsa-miR-99b#-002196	-4.26						

<https://doi.org/10.1371/journal.pone.0179645.t003>

Table 4. Differentially expressed miRNA in both types of clinical material by using two different normalization methods.

hsa-miR-126#-000451	hsa-miR-196b-002215	hsa-miR-21#-002438	hsa-miR-27a-000408
hsa-miR-140-3p-002234	hsa-miR-200b-002251	hsa-miR-210-000512	hsa-miR-29a-002112
hsa-miR-141-000463	hsa-miR-200c-002300	hsa-miR-224-002099	hsa-miR-452-002329
hsa-miR-143-002249	hsa-miR-205-000509	hsa-miR-27a#-002445	hsa-miR-886-3p-002194

<https://doi.org/10.1371/journal.pone.0179645.t004>

However, the improvement in the correlation when using non-dissected FFPE samples was due to a low number of samples which was not convincing [25]. In our analysis, we compared FF tumor samples with more than 50% of tumor cells and macrodissected FFPE tumor cells. Although, based on the PCA, the miRNA expression profiles differ between FF and FFPE, we performed the Spearman correlation test which showed a good correlation (Spearman correlation coefficient in the range from 0.65 to 0.84) in 70% of samples. Based on the study of de Biase et al. [25] who have pointed to the fact that dissection can influence the expression results which is necessary to take into account if the miRNA analysis is performed with or without dissection, we evaluated the correlation of the differentially expressed miRNAs in FF and FFPE based on the number of tumor cells in FF samples. However, no relationship between the number of tumor cells and correlation level was observed.

We revealed higher numbers of differentially regulated miRNAs in FF tonsillar tissues compared to the FFPE material which we attributed to the higher amount of RNA used for the miRNA expression analysis in FF samples. Therefore, some less expressed miRNAs could have been missed in FFPE samples. The overlap of differentially expressed miRNAs between FF and FFPE samples was around 30% which should be explained by the fact that unlike the tumor samples, the control non-malignant tissues were not paired between FF and FFPE and could influence the miRNA expression profiles more than we expected. Nevertheless, the analysis of both groups of tested material revealed the deregulation of the known tumor associated miRNAs such as miR-205, miR-210, or miRNAs from the family mir-8, as has been demonstrated in a number of solid tumors [29–32].

Further, when comparing the results obtained using two different types of data normalization, we revealed an overlap of between 58–67%. Therefore, the comparison between studies is obviously difficult because of the use of different methods of data analysis. In our analysis, both tissue types and both normalization methods overlap in 16 common miRNAs. All of these miRNAs were shown to be cancer related, nevertheless their role in head and neck cancer has not been elucidated. The role of miR-27a was mentioned by Venkatesh et al. as it regulates the expression of tumor suppressors in oral squamous cell carcinomas [33]. The role of miR-126# was found in endothelial proliferation [34, 35]. For miR-140-3p it was shown that it contributes to reduction of proliferation and migration of cancer cells in breast and lung cancer [36, 37] and in spinal chordoma, in contradictory, to be a marker of poor prognosis [38]. MiR-141 plays role in AKT signaling and inhibits prometastatic mesenchymal characteristics [39]. MiR-143 is a part of miR cluster 143/145 expressed in many tissues and regarded as tumor suppressing [40]. It's reduced expression was found also in cervical squamous cell carcinomas [41] and low expression of this miRNA contributes to poor prognosis in oral squamous cell carcinomas [42]. As recently discovered the expression of miR-196b promotes cell migration and invasion in oral cancer [43, 44]. Members of mir-200 family, which includes miR-200b, miR-200c and miR-205, are the major regulators of EMT pathway, primarily targeting transcriptional factors ZEB1 and SP1 [45], and play a prognostic role in various malignancies [46]. Deregulated expression of hypoxia-induced miR-210 was found in various tumors and influences cancer cell proliferation, apoptosis, angiogenesis and other cellular processes involved in

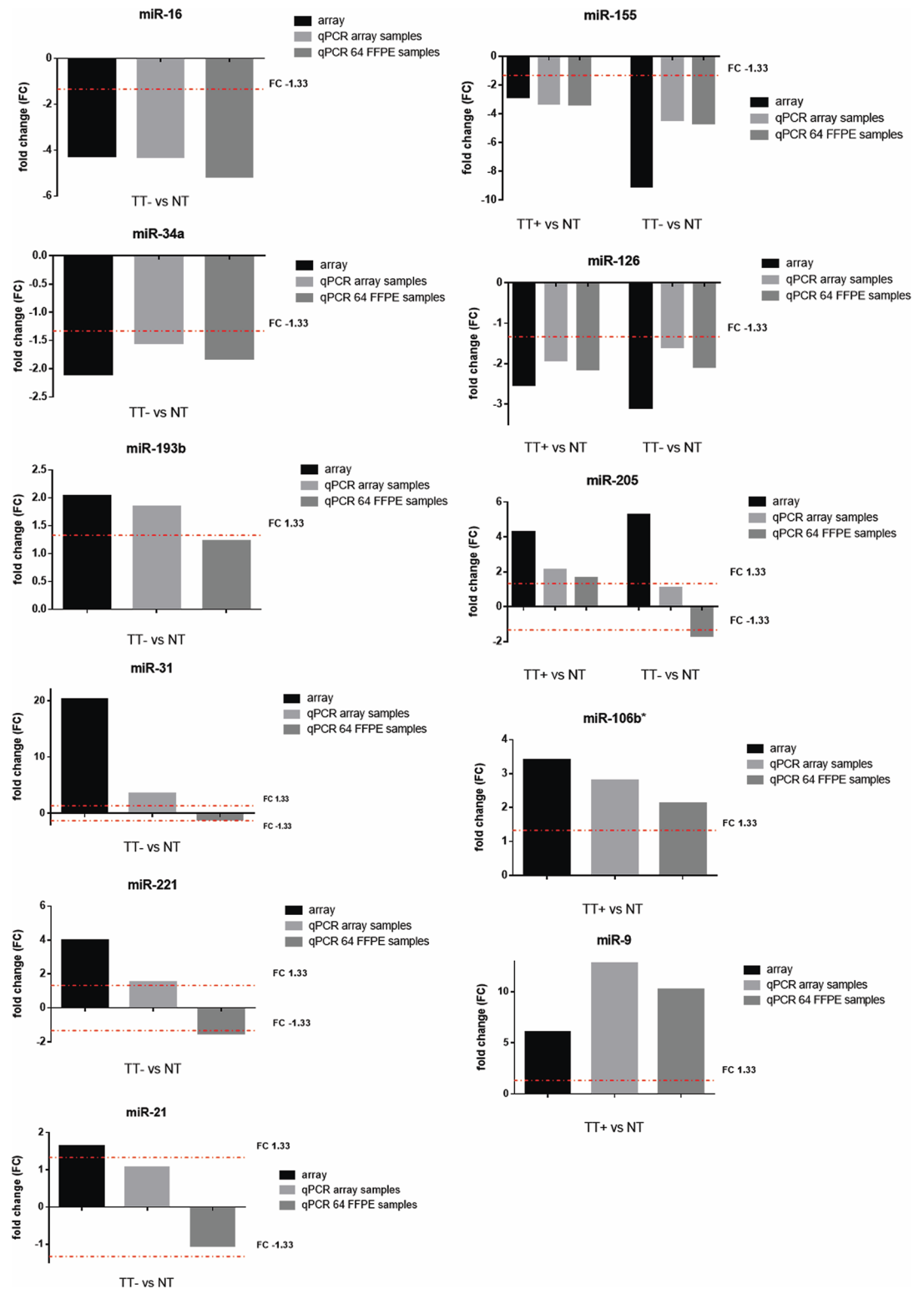


Fig 5. Comparison on fold-change for selected miRNAs between arrays and qPCR. The threshold of FC was set to 1.33. T-test or Mann Whitney nonparametric test was applied depending on the data distribution. All results were statistically significant ($P\text{-value} \leq 0.05$).

<https://doi.org/10.1371/journal.pone.0179645.g005>

tumor development [47]. The group of Seki et al. have been interested in the functional significance of mir-29 family, including miR-29a, in cervical cancer as well as in head and neck cancer. They found out that this tumor-suppressive miRNA inhibits cancer cell migration and invasion [48, 49]. Although some studies focused on the functional impact of identified miRNAs in HNC have been published, more extensive research is necessary to more accurately explain the relevance in HNC tumor development.

From the groups of deregulated miRNAs identified in FFPE tumors of either viral or non-viral etiology, we selected 11 miRNAs based on the results and relevance in the literature, the expression of which was evaluated in a larger set of 64 FFPE samples. From the group of miRNAs specific for HPV-positive tonsillar tumors, we choose upregulated miR-9 and miR-106b whose deregulation was previously reported in HNC [50–52]. Furthermore, miR-9 has been shown to be activated by HPV leading to increased cell motility [53] and to be involved in the pathways regulating metastasis [54]. Upregulated miR-31, miR-221, and miR-21 were selected for confirmation from the group of miRNAs specific for HPV-independent tumors including HNC as playing a role in increasing cell proliferation, invasion, and migration [55–58], participating in regulation of epithelial-mesenchymal transition (EMT), or having a prognostic impact [59, 60]. Further choices were miR-34a, specific for HPV-negative tumors, a tumor suppressor whose downregulation has been shown in a number of tumor types including HNC [61, 62], as well as miR-16, the inhibition of which promotes cell proliferation, migration, invasion, and EMT and contributes to tumor progression [63]. The last miRNA selected for confirmation from the group of HPV-negative tumors was miR-193b whose high expression in tissue was identified as an independent prognostic risk factor in patients with ovarian cancer [64]. From the group of tonsillar specific miRNAs regardless of the virus presence, we selected miR-205, miR-155, and miR-126 which participate in oncogenic pathways including cell proliferation, migration, or invasion and serve as prognostic predictors of patients with HNC [31, 65, 66].

We were able to confirm deregulated expression in the same set of samples as run on array. In this subset, deregulated expression was confirmed for all miRNAs except miR-21 and miR-205. However, their trend of expression was maintained and the fold change was close to the cut-off value. In the larger set of samples, deregulated expression was confirmed in 64% of comparisons. The fold change of miR-193b was equal to 1.23, and the trend of expression of four additional selected miRNAs was opposite to that revealed by arrays. The results suggest possible variability between samples and show that not all deregulated miRNAs detected in a smaller tested cohort might be representative of a broader spectrum of samples.

In conclusion, our study compares the miRNA expression profiles in tonsillar tumors as identified in fresh frozen and formalin-fixed paraffin-embedded samples. Although the correlation between the defined groups was relatively good for all miRNAs, the overlap of the selected differentially expressed miRNAs was rather suboptimal. We concluded that for accurate comparison between studies, the key factors are the use of the same type of clinical material and selection of the normalization method for data analysis. Additionally, we suggest that combining multiple analytical methods rather than a single test alone is advisable for more robust, reliable detection of differential abundance of miRNAs and interpretation of results.

Acknowledgments

The authors thank Blanka Langova and Stephanie Villar for technical assistance. Thanks are also due to the Institute of Pathological Physiology, 1st Faculty of Medicine, Charles University, Prague, for the opportunity to use their equipment for TLDA card analysis and to the

Genetics Services Platform of the International Agency for Research on Cancer for help with additional TLDA card processing.

The paper was supported by grant by the Ministry of Education, Youth and Sports of CR within the National Sustainability Program II (Project BIOCEV-FAR) LQ1604 and by the project “BIOCEV” (CZ.1.05/1.1.00/02.0109).

Author Contributions

Conceptualization: RT JZ.

Data curation: ZV JZ RT.

Formal analysis: ZV JZ RT.

Funding acquisition: RT.

Investigation: ZV MG JK.

Methodology: RT JZ.

Project administration: RT.

Resources: RT JZ MG JK.

Supervision: RT.

Validation: ZV JZ RT.

Visualization: ZV RT.

Writing – original draft: ZV JZ RT.

Writing – review & editing: ZV JZ MG JK RT.

References

1. Bartel DP. MicroRNAs: genomics, biogenesis, mechanism, and function. *Cell*. 2004; 116: 281–297. PMID: [14744438](https://pubmed.ncbi.nlm.nih.gov/14744438/)
2. Ørom UA, Nielsen FC, Lund AH. MicroRNA-10a binds the 5'UTR of ribosomal protein mRNAs and enhances their translation. *Mol Cell*. 2008; 30: 460–471. <https://doi.org/10.1016/j.molcel.2008.05.001> PMID: [18498749](https://pubmed.ncbi.nlm.nih.gov/18498749/)
3. Vasudevan S, Tong Y, Steitz JA. Switching from repression to activation: microRNAs can up-regulate translation. *Science*. 2007; 318: 1931–1934. <https://doi.org/10.1126/science.1149460> PMID: [18048652](https://pubmed.ncbi.nlm.nih.gov/18048652/)
4. Volinia S, Calin GA, Liu CG, Ambs S, Cimmino A, Petrocca F, et al. A microRNA expression signature of human solid tumors defines cancer gene targets. *Proc Natl Acad Sci USA*. 2006; 103: 2257–2261. <https://doi.org/10.1073/pnas.0510565103> PMID: [16461460](https://pubmed.ncbi.nlm.nih.gov/16461460/)
5. Jay C, Nemunaitis J, Chen P, Fulgham P, Tong AW. miRNA profiling for diagnosis and prognosis of human cancer. *DNA Cell Biol*. 2007; 26: 293–300. <https://doi.org/10.1089/dna.2006.0554> PMID: [17504025](https://pubmed.ncbi.nlm.nih.gov/17504025/)
6. Gao G, Gay HA, Chernock RD, Zhang TR, Luo J, Thorstad WL, et al. A microRNA expression signature for the prognosis of oropharyngeal squamous cell carcinoma. *Cancer*. 2013; 119: 72–80. <https://doi.org/10.1002/cncr.27696> PMID: [22736309](https://pubmed.ncbi.nlm.nih.gov/22736309/)
7. Wang X, Wang HK, Li Y, Hafner M, Banerjee NS, Tang S, et al. microRNAs are biomarkers of oncogenic human papillomavirus infections. *Proc Natl Acad Sci USA*. 2014; 111: 4262–4267. <https://doi.org/10.1073/pnas.1401430111> PMID: [24591631](https://pubmed.ncbi.nlm.nih.gov/24591631/)
8. Doleshal M, Magotra AA, Choudhury B, Cannon BD, Labourier E, Szafranska AE. Evaluation and validation of total RNA extraction methods for microRNA expression analyses in formalin-fixed, paraffin-embedded tissues. *J Mol Diagn*. 2008; 10: 203–211. <https://doi.org/10.2353/jmoldx.2008.070153> PMID: [18403610](https://pubmed.ncbi.nlm.nih.gov/18403610/)

9. Xi Y, Nakajima G, Gavin E, Morris CG, Kudo K, Hayashi K, Ju J. Systematic analysis of microRNA expression of RNA extracted from fresh frozen and formalin-fixed paraffin-embedded samples. *RNA*. 2007; 13: 1668–1674. <https://doi.org/10.1261/rna.642907> PMID: 17698639
10. Jung M, Schaefer A, Steiner I, Kempkensteffen C, Stephan C, Erbersdobler A, Jung K. Robust micro-RNA stability in degraded RNA preparations from human tissue and cell samples. *Clin Chem*. 2010; 56: 998–1006. <https://doi.org/10.1373/clinchem.2009.141580> PMID: 20378769
11. Vojtechova Z, Sabol I, Salakova M, Smahelova J, Zavadil J, Turek L, et al. Comparison of the miRNA profiles in HPV-positive and HPV-negative tonsillar tumors and a model system of human keratinocyte clones. *BMC Cancer*. 2016; 16: 382. <https://doi.org/10.1186/s12885-016-2430-y> PMID: 27377959
12. Hui AB, Shi W, Boutros PC, Miller N, Pintilie M, Fyles T, et al. Robust global micro-RNA profiling with formalin-fixed paraffin-embedded breast cancer tissues. *Lab Invest*. 2009; 9: 597–606.
13. Goswami RS, Waldron L, Machado J, Cervigne NK, Xu W, Reis PP, et al. Optimization and analysis of a quantitative real-time PCR-based technique to determine microRNA expression in formalin-fixed paraffin-embedded samples. *BMC Biotechnol*. 2010; 10: 47. <https://doi.org/10.1186/1472-6750-10-47> PMID: 20573258
14. Romero-Cordoba S, Rodriguez-Cuevas S, Rebollar-Vega R, Quintanar-Jurado V, Maffuz-Aziz A, Jimenez-Sanchez G, et al. Identification and pathway analysis of microRNAs with no previous involvement in breast cancer. *PLoS One*. 2012; 7: e31904. <https://doi.org/10.1371/journal.pone.0031904> PMID: 22438871
15. Vojtechova Z, Sabol I, Salakova M, Turek L, Grega M, Smahelova J, et al. Analysis of the integration of human papillomaviruses in head and neck tumours in relation to patients' prognosis. *Int J Cancer*. 2016; 138: 386–395. <https://doi.org/10.1002/ijc.29712> PMID: 26239888
16. Osawa S, Shimada Y, Sekine S, Okumura T, Nagata T, Fukuoka J, et al. MicroRNA profiling of gastric cancer patients from formalin-fixed paraffin-embedded samples. *Oncol Lett*. 2011; 2: 613–619.
17. Lee TS, Jeon HW, Kim YB, Kim YA, Kim MA, Kang SB, et al. Aberrant microRNA expression in endometrial carcinoma using formalin-fixed paraffin-embedded (FFPE) tissues. *PLoS One*. 2013; 8: e81421. <https://doi.org/10.1371/journal.pone.0081421> PMID: 24363810
18. Ganci F, Sacconi A, Manciooco V, Sperduti I, Battaglia P, Covello R, et al. MicroRNA expression profiling of thymic epithelial tumors. *Lung Cancer*. 2014; 5: 197–204.
19. Leichter AL, Purcell RV, Sullivan MJ, Eccles MR, Chatterjee A. Multi-platform microRNA profiling of hepatoblastoma patients using formalin fixed paraffin embedded archival samples. *Gigascience*. 2015; 4: 54. <https://doi.org/10.1186/s13742-015-0099-9> PMID: 26613016
20. Chatterjee A, Leichter AL, Fan V, Tsai P, Purcell RV, Sullivan MJ, et al. A cross comparison of technologies for the detection of microRNAs in clinical FFPE samples of hepatoblastoma patients. *Sci Rep*. 2015; 5: 10438. <https://doi.org/10.1038/srep10438> PMID: 26039282
21. Li J, Smyth P, Flavin R, Cahill S, Denning K, Aherne S, et al. Comparison of miRNA expression patterns using total RNA extracted from matched samples of formalin-fixed paraffin-embedded (FFPE) cells and snap frozen cells. *BMC Biotechnol*. 2007; 7: 36. <https://doi.org/10.1186/1472-6750-7-36> PMID: 17603869
22. Hoefig KP, Thorns C, Roehle A, Kaehler C, Wesche KO, Reipsilber D, et al. Unlocking pathology archives for microRNA-profiling. *Anticancer Res*. 2008; 28: 119–123. PMID: 18383833
23. Mortarino M, Gioia G, Gelain ME, Albonico F, Roccabianca P, Ferri E, et al. Identification of suitable endogenous controls and differentially expressed microRNAs in canine fresh-frozen and FFPE lymphoma samples. *Leuk Res*. 2010; 34: 1070–1077. <https://doi.org/10.1016/j.leukres.2009.10.023> PMID: 19945163
24. Leite KR, Canavez JM, Reis ST, Tomiyama AH, Piantino CB, Sañudo A, et al. miRNA analysis of prostate cancer by quantitative real time PCR: comparison between formalin-fixed paraffin embedded and fresh-frozen tissue. *Urol Oncol*. 2011; 29: 533–537. <https://doi.org/10.1016/j.urolonc.2009.05.008> PMID: 19734068
25. de Biase D, Visani M, Morandi L, Marucci G, Taccioli C, Cerasoli S, et al. miRNAs expression analysis in paired fresh/frozen and dissected formalin fixed and paraffin embedded glioblastoma using real-time pCR. *PLoS One*. 2012; 7: e35596. <https://doi.org/10.1371/journal.pone.0035596> PMID: 22530056
26. Zhang X, Chen J, Radcliffe T, Lebrun DP, Tron VA, Feilotter H, et al. An array-based analysis of micro-RNA expression comparing matched frozen and formalin-fixed paraffin-embedded human tissue samples. *J Mol Diagn*. 2008; 10: 513–519. <https://doi.org/10.2353/jmoldx.2008.080077> PMID: 18832457
27. Glud M, Klausen M, Gniadecki R, Rossing M, Hastrup N, Nielsen FC, et al. MicroRNA expression in melanocytic nevi: the usefulness of formalin-fixed, paraffin-embedded material for miRNA microarray profiling. *J Invest Dermatol*. 2009; 129: 1219–1224. <https://doi.org/10.1038/jid.2008.347> PMID: 19005486

28. Meng W, McElroy JP, Volinia S, Palatini J, Warner S, Ayers LW, et al. Comparison of microRNA deep sequencing of matched formalin-fixed paraffin-embedded and fresh frozen cancer tissues. *PLoS One*. 2013; 8: e64393. <https://doi.org/10.1371/journal.pone.0064393> PMID: 23696889
29. Gee HE, Camps C, Buffa FM, Patiar S, Winter SC, Betts G, et al. Hsa-Mir-210 is a Marker of Tumor Hypoxia and a Prognostic Factor in Head and Neck Cancer. *Cancer*. 2010; 116: 2148–2158. <https://doi.org/10.1002/cncr.25009> PMID: 20187102
30. Gao Y, Feng B, Han S, Zhang K, Chen J, Li C, et al. The Roles of MicroRNA-141 in Human Cancers: From Diagnosis to Treatment. *Cell Physiol Biochem*. 2016; 38: 427–448. <https://doi.org/10.1159/000438641> PMID: 26828359
31. Mao Y, Wu S, Zhao R, Deng Q. MiR-205 promotes proliferation, migration and invasion of nasopharyngeal carcinoma cells by activation of AKT signalling. *J Int Med Res*. 2016; 44: 231–240. <https://doi.org/10.1177/0300060515576556> PMID: 26880795
32. Zeng F, Xue M, Xiao T, Li Y, Xiao S, Jiang B, et al. MiR-200b promotes the cell proliferation and metastasis of cervical cancer by inhibiting FOXG1. *Biomed Pharmacother*. 2016; 79: 294–301. <https://doi.org/10.1016/j.biopha.2016.02.033> PMID: 27044840
33. Venkatesh T, Nagashri MN, Swamy SS, Mohiyuddin SM, Gopinath KS, Kumar A. Primary microcephaly gene MCPH1 shows signatures of tumor suppressors and is regulated by miR-27a in oral squamous cell carcinoma. *Plos One* 2013; 8: e54643. <https://doi.org/10.1371/journal.pone.0054643> PMID: 23472065
34. Zhang Y, Song H, Zhang Y, Wu F, Mu Q, Jiang M, et al. Irisin inhibits atherosclerosis by promoting endothelial proliferation through microRNA126-5p. *J Am Heart Assoc*. 2016;5.
35. Schober A, Nazari-Jahantigh M, Wei Y, Bidzhekov K, Gremse F, Grommes J, et al. MicroRNA-126-5p promotes endothelial proliferation and limits atherosclerosis by suppressing Dlk1. *Nat Med* 2014; 20: 368–76. <https://doi.org/10.1038/nm.3487> PMID: 24584117
36. Salem O, Erdem N, Jung J, Münstermann E, Wörner A, Wilhelm H, et al. The highly expressed 5'isomiR of hsa-miR-140-3p contributes to the tumor-suppressive effects of miR-140 by reducing breast cancer proliferation and migration. *BMC Genomics* 2016; 17: 566. <https://doi.org/10.1186/s12864-016-2869-x> PMID: 27502506
37. Kong XM, Zhang GH, Huo YK, Zhao XH, Cao DW, Guo SF, et al. MicroRNA-140-3p inhibits proliferation, migration and invasion of lung cancer cells by targeting ATP6AP2. *Int J Clin Exp Pathol* 2015; 8: 12845–52. PMID: 26722475
38. Zou MX, Huang W, Wang XB, Lv GH, Li J, Deng YW. Identification of miR-140-3p as a marker associated with poor prognosis in spinal chordoma. *Int J Clin Exp Pathol* 2014; 7: 4877–85. PMID: 25197358
39. Al-Khalaf HH and Aboussekhra A. MicroRNA-141 and microRNA-146b-5p inhibit the prometastatic mesenchymal characteristics through the RNA-binding Protein AUF1 targeting the transcription factor ZEB1 and the protein kinase AKT. *J Biol Chem* 2014; 289: 31433–31447. <https://doi.org/10.1074/jbc.M114.593004> PMID: 25261470
40. Das AV and Pillai RM. Implications of miR cluster 143/145 as universal anti-oncomiRs and their dysregulation during tumorigenesis. *Cancer Cell Int* 2015; 15: 92. <https://doi.org/10.1186/s12935-015-0247-4> PMID: 26425114
41. Chen Y, Ma C, Zhang W, Chen Z, Ma L. Down regulation of miR-143 is related with tumor size, lymph node metastasis and HPV16 infection in cervical squamous cancer. *Diagn Pathol* 2014; 9: 88. <https://doi.org/10.1186/1746-1596-9-88> PMID: 24774218
42. Bufalino A, Cervigne NK, de Oliveira CE, Fonseca FP, Rodrigues PC, Macedo CC, et al. Low miR-143/miR-145 cluster levels induce activin A overexpression in oral squamous cell carcinomas, which contributes to poor prognosis. *Plos One* 2015; 10: e0136599. <https://doi.org/10.1371/journal.pone.0136599> PMID: 26317418
43. Lu YC, Chang JT, Liao CT, Kang CJ, Huang SF, Chen IH, et al. OncomiR-196 promotes an invasive phenotype in oral cancer through the NME4-JNK-TIMP1-MMP signaling pathway. *Mol Cancer* 2014; 13: 218. <https://doi.org/10.1186/1476-4598-13-218> PMID: 25233933
44. Hou YY, You JJ, Yang CM, Pan HW, Chen HC, Lee JH, et al. Aberrant DNA hypomethylation of miR-196b contributes to migration and invasion of oral cancer. *Oncol Lett* 2016; 11: 4013–4021. <https://doi.org/10.3892/ol.2016.4491> PMID: 27313732
45. Gregory PA, Bert AG, Paterson EL, Barry SC, Tsykin A, Farshid G, et al. The miR-200 family and miR-205 regulate epithelial to mesenchymal transition by targeting ZEB1 and SP1. *Nat Cell Biol* 2008; 10: 593–601. <https://doi.org/10.1038/ncb1722> PMID: 18376396
46. Zhang KC, Xi HQ, Cui JX, Shen WS, Li JY, Wei B, et al. Prognostic role of miR-200c in various malignancies: a systematic review and meta-analysis. *Int J Clin Exp Med* 2015; 8: 1931–43. PMID: 25932122
47. Qin Q, Furong W, Baosheng L. Multiple functions of hypoxia-regulated miR-210 in cancer. *J Exp Clin Cancer Res* 2014; 33: 50. <https://doi.org/10.1186/1756-9966-33-50> PMID: 24909053

48. Yamamoto N, Kinoshita T, Nohata N, Yoshino H, Itesako T, Fujimura L, et al. Tumor-suppressive microRNA-29a inhibits cancer cell migration and invasion via targeting HSP47 in cervical squamous cell carcinoma. *Int J Oncol* 2013; 43: 1855–63. <https://doi.org/10.3892/ijo.2013.2145> PMID: 24141696
49. Kinoshita T, Nohata N, Hanazawa T, Kikkawa N, Yamamoto N, Yoshino H, et al. Tumour-suppressive microRNA-29s inhibit cancer cell migration and invasion by targeting laminin–integrin signalling in head and neck squamous cell carcinoma. *Br J Cancer* 2013; 109: 2636–45. <https://doi.org/10.1038/bjc.2013.607> PMID: 24091622
50. Hui AB, Lin A, Xu W, Waldron L, Perez-Ordóñez B, Weinreb I, et al. Potentially prognostic miRNAs in HPV-associated oropharyngeal carcinoma. *Clin Cancer Res*. 2013; 19: 2154–2162. <https://doi.org/10.1158/1078-0432.CCR-12-3572> PMID: 23459718
51. Lu ZM, Lin YF, Jiang L, Chen LS, Luo XN, Song XH, et al. Micro-ribonucleic acid expression profiling and bioinformatic target gene analyses in laryngeal carcinoma. *Onco Targets Ther*. 2014; 7: 525–533. <https://doi.org/10.2147/OTT.S59871> PMID: 24741319
52. Miller DL, Davis JW, Taylor KH, Johnson J, Shi Z, Williams R, et al. Identification of a human papillomavirus-associated oncogenic miRNA panel in human oropharyngeal squamous cell carcinoma validated by bioinformatics analysis of the Cancer Genome Atlas. *Am J Pathol*. 2015; 185: 679–692. <https://doi.org/10.1016/j.ajpath.2014.11.018> PMID: 25572154
53. Liu W, Gao G, Hu X, Wang Y, Schwarz JK, Chen JJ, et al. Activation of miR-9 by human papillomavirus in cervical cancer. *Oncotarget*. 2014; 5: 11620–11630. <https://doi.org/10.18632/oncotarget.2599> PMID: 25344913
54. Zhu L, Chen H, Zhou D, Li D, Bai R, Zheng S, et al. MicroRNA-9 up-regulation is involved in colorectal cancer metastasis via promoting cell motility. *Med Oncol*. 2012; 29: 1037–1043. <https://doi.org/10.1007/s12032-011-9975-z> PMID: 21562850
55. Siow MY, Ng LP, Vincent-Chong VK, Jamaludin M, Abraham MT, Abdul Rahman ZA, et al. Dysregulation of miR-31 and miR-375 expression is associated with clinical outcomes in oral carcinoma. *Oral Dis*. 2014; 20: 345–351. <https://doi.org/10.1111/odi.12118> PMID: 23651447
56. He S, Lai R, Chen D, Yan W, Zhang Z, Liu Z, et al. Downregulation of miR-221 Inhibits Cell Migration and Invasion through Targeting Methyl-CpG Binding Domain Protein 2 in Human Oral Squamous Cell Carcinoma Cells. *Biomed Res Int*. 2015; 751672. <https://doi.org/10.1155/2015/751672> PMID: 26788506
57. Wang L, Liu C, Li C, Xue J, Zhao S, Zhan P, et al. Effects of microRNA-221/222 on cell proliferation and apoptosis in prostate cancer cells. *Gene*. 2015; 572: 252–258. <https://doi.org/10.1016/j.gene.2015.07.017> PMID: 26164758
58. Zhu J, Liu F, Wu Q, Liu X. MiR-221 increases osteosarcoma cell proliferation, invasion and migration partly through the downregulation of PTEN. *Int J Mol Med*. 2015; 36: 1377–1383. <https://doi.org/10.3892/ijmm.2015.2352> PMID: 26397386
59. Ko YH, Won HS, Sun DS, An HJ, Jeon EK, Kim MS, et al. Human papillomavirus-stratified analysis of the prognostic role of miR-21 in oral cavity and oropharyngeal squamous cell carcinoma. *Pathol Int*. 2014; 64: 499–507. <https://doi.org/10.1111/pin.12201> PMID: 25236707
60. Sun SS, Zhou X, Huang YY, Kong LP, Mei M, Guo WY, et al. Targeting STAT3/miR-21 axis inhibits epithelial-mesenchymal transition via regulating CDK5 in head and neck squamous cell carcinoma. *Mol Cancer*. 2015; 14: 213. <https://doi.org/10.1186/s12943-015-0487-x> PMID: 26690371
61. Kumar B, Yadav A, Lang J, Teknos TN, Kumar P. Dysregulation of microRNA-34a expression in head and neck squamous cell carcinoma promotes tumor growth and tumor angiogenesis. *PLoS One*. 2012; 7: e37601. <https://doi.org/10.1371/journal.pone.0037601> PMID: 22629428
62. Jia LF, Wei SB, Mitchelson K, Gao Y, Zheng YF, Meng Z, et al. miR-34a inhibits migration and invasion of tongue squamous cell carcinoma via targeting MMP9 and MMP14. *PLoS One*. 2014; 9: e108435. <https://doi.org/10.1371/journal.pone.0108435> PMID: 25268950
63. Renjie W and Haiqian L. MiR-132, miR-15a and miR-16 synergistically inhibit pituitary tumor cell proliferation, invasion and migration by targeting Sox5. *Cancer Lett*. 2015; 356: 568–578. <https://doi.org/10.1016/j.canlet.2014.10.003> PMID: 25305447
64. Li H, Xu Y, Qiu W, Zhao D, Zhang Y. Tissue miR-193b as a Novel Biomarker for Patients with Ovarian Cancer. *Med Sci Monit*. 2015; 21: 3929–3934. <https://doi.org/10.12659/MSM.895407> PMID: 26675282
65. Sasahira T, Kurihara M, Bhawal UK, Ueda N, Shimomoto T, Yamamoto K, et al. Downregulation of miR-126 induces angiogenesis and lymphangiogenesis by activation of VEGF-A in oral cancer. *Br J Cancer*. 2012; 107: 700–706. <https://doi.org/10.1038/bjc.2012.330> PMID: 22836510
66. Lerner C, Wemmert S, Bochen F, Kulas P, Linxweiler M, Hasenfus A, et al. Characterization of miR-146a and miR-155 in blood, tissue and cell lines of head and neck squamous cell carcinoma patients and their impact on cell proliferation and migration. *J Cancer Res Clin Oncol*. 2016; 142: 757–766. <https://doi.org/10.1007/s00432-015-2087-y> PMID: 26621153